

Activation of the P2X₇ receptor in midbrain periaqueductal gray participates in the analgesic effect of tramadol in bone cancer pain rats

Pengtao Li¹, Quan Zhang^{2,3}, Zhi Xiao^{2,3}, Shouyang Yu², Yan Yan^{2,3}, and Ying Qin³

Molecular Pain
Volume 14: 1–14
© The Author(s) 2018
Article reuse guidelines:
sagepub.com/journals-permissions
DOI: 10.1177/1744806918803039
journals.sagepub.com/home/mpx


Abstract

Background: Cancer pain is a well-known serious complication in metastatic or terminal cancer patients. Current pain management remains unsatisfactory. The activation of spinal and supraspinal P2X₇ receptors plays a crucial role in the induction and maintenance mechanisms of various kinds of acute or chronic pain. The midbrain periaqueductal gray is a vital supraspinal site of the endogenous descending pain-modulating system. Tramadol is a synthetic, centrally acting analgesic agent that exhibits considerable efficacy in clinically relieving pain. The purpose of this study was to determine whether the activation of P2X₇ receptor in the ventrolateral region of the periaqueductal gray (vIPAG) participates in the analgesic mechanisms of tramadol on bone cancer pain in rats. The bone cancer pain rat model was established by intratibial cell inoculation of SHZ-88 mammary gland carcinoma cells. The analgesic effects of different doses of tramadol (10, 20, and 40 mg/kg) were assessed by measuring the mechanical withdrawal threshold and thermal withdrawal latency values in rats by using an electronic von Frey anesthesiometer and radiant heat stimulation, respectively. Alterations in the number of P2X₇ receptor-positive cells and P2X₇ protein levels in vIPAG were separately detected by using immunohistochemistry and Western blot assay. The effect of intra-vIPAG injection of A-740003 (100 nmol), a selective competitive P2X₇ receptor antagonist, on the analgesic effect of tramadol was also observed.

Results: The expression of P2X₇ receptor in the vIPAG on bone cancer pain rats was mildly elevated, and the tramadol (10, 20, and 40 mg/kg) dose dependently relieved pain-related behaviors in bone cancer pain rats and further upregulated the expression of P2X₇ receptor in the vIPAG. The intra-vIPAG injection of A-740003 pretreatment partly but significantly antagonized the analgesic effect of tramadol on bone cancer pain rats.

Conclusions: The injection of tramadol can dose dependently elicit analgesic effect on bone cancer pain rats by promoting the expression of the P2X₇ receptor in vIPAG.

Keywords

Bone cancer pain, tramadol, midbrain periaqueductal gray, P2X₇ receptor, analgesic effect

Date Received: 19 June 2018; revised: 21 July 2018; accepted: 28 August 2018

Background

Bone cancer pain (BCP) is the most common cancer pain arises from bone metastasis of malignant tumors like breast, prostate, and lung cancers.^{1,2} BCP patients frequently experience daily pain that substantially impairs their quality of life.^{3,4} With the rapid increase in the incidence and survival rates of cancer and prolonged survival of patients, finding strategies to manage BCP has become increasingly important.³ Unfortunately, the neural

¹Graduate School, Zunyi Medical University, Zunyi, Guizhou, China

²Key Laboratory of Brain Science, Zunyi Medical University, Zunyi, Guizhou, China

³Research Center for Medicine and Biology, Zunyi Medical University, Zunyi, Guizhou, China

The first two authors contributed equally to this work.

Corresponding Author:

Zhi Xiao, Key Laboratory of Brain Science, Zunyi Medical University, No.6 West Xuefu Road, Xindu District, Zunyi, Guizhou, China.

Email: xiaozhi1971@163.com



mechanisms underpinning BCP are still remain unsolved.⁵ From the basic research point of view, pathological phenotypes, such as neuropathic and inflammatory pain, are the underlying components of BCP,⁶ thus making BCP a well-known complex pain state. Numerous studies have shown that neuronal and/or glial cell function, pain-related neurotransmitters, receptors, and proinflammatory cytokines are all major factors linked to the molecular mechanisms of BCP.^{7–12}

At present, cancer pain is commonly managed using a “three-step” analgesic ladder, which was originally developed by the World Health Organization in 1986; this ladder involves opioids and non-opioid analgesics (nonsteroidal anti-inflammatory drugs).³ Other adjuvant therapies, including radiation therapy, surgery, and chemotherapy, are also used to control cancer pain.³ However, current therapies are often partially effective because of their relative ineffectiveness and severe side effects, such as tolerance, withdrawal, dependence, and addiction to opioids.⁴ Studies have shown that almost half of cancer pain is not adequately relieved and that BCP is one of the most debilitating conditions to treat.^{3,13} Thus, new analgesic therapies that are efficacious and/or capable of abating the side effects of current therapies should be developed.

Adenosine triphosphate (ATP) is a widely distributed signaling molecule.¹⁴ ATP activates a vast variety of pathways, allowing downstream effects that can lead to both physiological and pathological responses in the central/peripheral nervous system via activation of the P2X and P2Y receptors.¹⁵ At present, the pathophysiology and therapeutic potential of P2X receptors are the focus of basic research and clinical treatment. Among all P2X receptors, the P2X₇ receptor is a well-defined therapeutic target for a series of diseases that has been found in the central and peripheral nervous systems.^{16–19} Numerous studies have shown that P2X₇ receptor is a key factor responsible for the occurrence and development of neuropathic pain and inflammatory pain.^{20–22}

The neuronal circuit and endogenous substances construct a presumptive endogenous nociceptive modulatory system that originates from the anterior cingulate cortex or hypothalamus to the midbrain periaqueductal gray (PAG) and the ventromedial medulla (VMM): detected; and terminates in the spinal cord (dorsal horn).^{23,24} PAG is a deciding site in this modulatory system, which involves the integration of somatic and autonomic responses to nociceptive and other stressful stimuli.²⁵ When stimulated by electrical or excitatory amino acids, PAG integrates descending noradrenergic and serotonergic pathway activity, which can suppress nociceptive transmission from the dorsal horn of the spinal cord; this phenomenon suggests that changes in PAG may be a common feature in different pain models. The ventrolateral region of the periaqueductal gray

(vlPAG) is a particularly important site in descending control of nociception.^{25,26} Early studies revealed that P2X₁₋₆ receptors exist in PAG,²⁷ and subsequent investigations confirmed that the P2X₇ receptor can be added to this archive.^{28,29}

Tramadol hydrochloride, (1RS, 2RS)-2-[(dimethylamino)methyl]-1-(3-methoxyphenyl)-cyclohexanol (HCl), is an atypical central opioid receptor analgesic prescribed to relieve moderate to severe pain caused by numerous different illnesses and diseases, such as inflammatory, cancer, neuropathic, and postoperative pain.^{30–32} Drug addiction, respiratory depression, drug abuse, and other side effects of this drug are trivial.³³ Different from classic opioids, tramadol exhibits dual analgesic mechanisms, namely, central and peripheral mechanisms. In brief, the mechanism of central analgesic effect occurs through the activation of the mu opioid receptors or reduction of norepinephrine (NE) and 5-hydroxytryptamine (5-HT) reabsorption, whereas the peripheral mechanism is a local anesthetic effect.^{34,35} To the best of our knowledge, the role of the vlPAG P2X₇ receptor in the mechanisms of tramadol analgesia has yet to be reported; therefore, the main purpose of this study is to observe the analgesic effect of tramadol on BCP rats and elucidate whether vlPAG P2X₇ receptor is involved in the underlying mechanisms. This study is expected to enhance our understanding of the mechanisms of supraspinal pain modulation and provide theoretical support for tramadol clinical analgesia.

Methods

Animals and ethics

Female Sprague–Dawley rats weighing 210 ± 10 g at the beginning of the experiments were purchased from the Laboratory Animal Center of the Army Medical University (Chongqing, China) and used for all experiments. The animals were housed in groups of five in a polypropylene cage with a 12 h light–dark cycle (8:00 a.m.–8:00 p.m.). The laboratory conditions were $25^{\circ}\text{C} \pm 2^{\circ}\text{C}$ and $55\% \pm 5\%$ relative humidity. Food and water were provided ad libitum. All experimental procedures were conducted according to the guidelines of the Ethical Committee of the International Association for the Study of Pain,³⁶ and the Animal Care Ethics Committee of Zunyi Medical University approved all the experimental protocols. Efforts were made to minimize the number of animals used and reduce their chances of suffering from experimental procedures.

Preparation of cancer cells

SHZ-88 mammary gland carcinoma cells were purchased commercially from the Shanghai Cell Bank of

the Chinese Academy of Sciences (Shanghai, China) and cultured in Roswell Park Memorial Institute (RPMI)-1640 medium (Sangon Biotech, Shanghai, China) in a 37°C constant-temperature incubator (Thermo, USA) containing 5% CO₂. The cell culture medium was changed every two days, and cell passage was conducted every week. In order to detach, the cultured cells were digested by 0.25% trypsin for 5–8 min, and the enzyme reaction was terminated with a culture medium containing 10% fetal bovine serum. For cells harvesting, the cells and medium were centrifuged for 3 min at 1000 r/min. The supernatant thus obtained was discarded and the pellet resuspended in the RPMI-1640 medium and diluted to achieve a final concentration of 10⁷ cells/0.5 mL. The cells were counted by using a hemocytometer. Cell viability was estimated by MTT ((3-[4,5-dimethylthiazol-2-yl]-2,5 diphenyl tetrazolium bromide)) assay as described previously.³⁷

Model of cancer pain

All animals were assessed for their baseline nociceptive sensitivity to mechanical and thermal stimuli one day prior to experiments. Only the animals with normal baseline responses were used in the study. BCP model was conducted as described previously.³⁸ In brief, under 4% chloral hydrate anesthesia (10 mL/kg body weight, intraperitoneal, i.p.), this method provided a state of anesthesia with stable physiological parameters. The rats were placed in a prone position on a thermo-regulated heat mat. A 1.5-cm incision was made on the right leg of the rat to expose the upper medial aspect of the tibia with minimal damage to the muscles and nerves, and 20 µL of SHZ-88 carcinoma cells (10⁷ cells/0.5 mL) was slowly injected into the intramedullary cavity of the tibia. The syringe was removed, and the injection site was immediately closed with sterile bone wax. Then, penicillin was applied to the wound. In the sham-BCP group, the same procedures were followed, except that cancer cells at an equal volume and concentration were heated to 90°C for 20 min and administered instead of normal carcinoma cells. The day of carcinoma cells inoculation is day 0.

Bone radiological detection

Bone radiological detection was assessed on day 21 prior to decalcification and histological staining. After anesthesia with injection of 4% chloral hydrate (10 mL/kg body weight, i.p.), the hind limb of the rat was exposed to an intraoral X-ray source for 0.32 s at 60 kV, 7 mA (Kodak, CS2200, Carestream Health, Inc.). The bone destruction of each proximal tibia was detected based on the blind analysis of radiographs.

Hematoxylin–eosin staining

Histological staining was conducted as described previously with minor alterations³⁹; fresh rat tibial tissue was gently separated, rinsed in 0.9% sodium chloride, and fixed in 4% paraformaldehyde for 12 h. These steps were followed by decalcification in 6.5% nitric acid/10% formaldehyde solution for 12 h. The decalcification process was terminated when the bone was easily penetrated through by a needle without any force, followed by routine dehydration and paraffin embedding. Several 3 µm sections were cut using a microtome (REM-710, YAMATO, Japan) and placed on clean glass slides. The sections were stained with hematoxylin solution for 5 min and then rinsed with distilled water. The sections were stained with eosin solution for 2 min, dehydrated with graded alcohol, and cleared with xylene. The mounted slides were then examined and photographed using a light microscope (IX53+DP73, OLYMPUS, Japan). Analysis was performed in a blinded manner.

Cannula implant and microinjection procedures

After anesthesia with injection of 4% chloral hydrate (10 mL/kg body weight, i.p.), the rats were mounted on a stereotaxic frame (68025, RWD Life Science Co., Ltd, Shenzhen, China). The skull was exposed and the bregma was located. A stainless steel guide cannula (0.48 mm outside diameter (O.D.) 0.34 mm inner diameter (I.D.)) was fixed to the skull by using dental zinc cement and jewelers' screw. Stereotaxic coordinates for vIPAG were 7.90 mm posterior to the bregma, 0.80 mm lateral to the midline, and 6.00 mm ventral to the skull surface. A dummy cannula inserted into the guide cannula at the time of surgery served to reduce the incidence of occlusion. Upon removal from stereotaxic apparatus, rats were administered with 2 mL of 0.9% sterile saline s.c. to prevent dehydration and placed in a thermal-controlled cage to prevent hypothermia until complete anesthetic recovery. Prior to any experimentation, the animals were allowed to recover from implantation surgery for four days at minimum, and signs of motor deficiency were monitored daily. Rats with neurological deficits resulting from the surgical procedure were excluded from the experiments. On the day of microinjection, the rats were transferred from the main holding area to the laboratory and left undisturbed for 1 h prior to drug administration. Each rat was lightly restrained and inserted with an injection cannula (0.3 mm O.D.; 0.5 mm longer than the guide cannula) into the guide cannula and an injector connected to a micro-injection pump (Legato 130, KD Scientific, USA). A total volume of 0.3 µL was injected over a 3-min period, and the injector remained in place for an additional 1 min before slow removal to ensure complete diffusion of

the drug. At the end of the experiments, the animals were deeply anesthetized by an injection of a 4% chloral hydrate (20 mL/kg body weight, i.p) and intracardially perfused with physiological saline (0.9% NaCl) followed by 4% paraformaldehyde solution. The position of the cannula was visually confirmed by 0.1 μ L of 2% Evans blue infusion through the microinjection cannula at the end of the experiment. Administration sites were verified by histological examination and plotted on coronal maps adapted from the atlas of Paxinos and Watson as a reference.⁴⁰ Only rats with microinjection site located within vIPAG were used for analysis (Figure 1).

Inclined plane test

The functional deficit of locomotion, including muscular strength and proprioception, was evaluated using an inclined plane according to a previously reported method.⁴¹ The rats were placed crosswise to the long axis of an inclined plane. The initial angle of the inclined plane was 30°, and the angle was tilted slowly by 5° increments. The maximum angle of the plane on which the rats maintained a constant body position for 5 s without falling was recorded. This measurement was recorded for five times for each rat, and the average values from the measurements were defined as the inclined plane test values.

The electronic pressure meter test of mechanical withdrawal threshold

For determining mechanical withdrawal thresholds (MWTs) in a quiet room, each rat was placed in an individual Plexiglass house (18 cm \times 12 cm \times 12 cm) with a

wire mesh floor and allowed to explore and groom until they settled down. Each hind paw was measured for five times, and the average values from the measurements were considered as the mechanical paw withdrawal thresholds. Mechanical hyperalgesia was tested in rats as reported previously.⁴² In brief, the test consists of evoking hind paw flexion reflex with the electronic von Frey anesthesiometer (IITC Life Science Instruments, USA) adapted with a 0.5 mm² contact area polypropylene tip. The investigator was trained to apply the tip perpendicularly to the central area of the hind paw with a gradual increase in pressure, and the endpoint was characterized by the removal of the paw (the animal actively lifted the whole paw upon the tip of the anesthesiometer, bit or licked the paw, or shook the paw with high amplitude movements in response to the stimulus).

Radiant heat test

Radiant heat test described by Hargreaves et al.⁴³ was carried out to evaluate thermal withdrawal latency (TWL). In brief, each rat was placed in a clean plastic chamber, allowed to adapt for 30 min, and exploratory behavior ceased. Then, 52°C \pm 0.2°C radiant heat (50 W, 8 V bulb) was applied to the plantar surface of the hind paw. The latency period was recorded between the start of the beam and a functional response, namely, characteristic lifting, hind paw licking, flicking, or commenced jumping. For preventing tissue injury, the cut-off limit was set to 60 s. Each hind paw was measured for three times at 3-min intervals. The average value from three measurements was considered as the value of TWL.

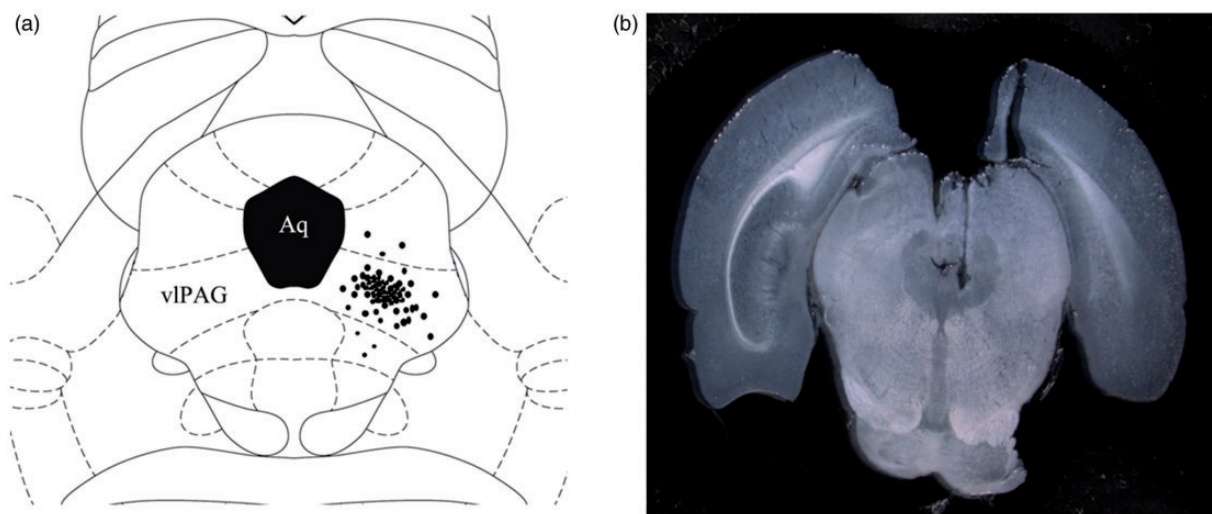


Figure 1. (a) Schematic diagram illustrates the sites of A-740003 microinjections, which were identified histologically by Evans blue dye microinjection (dots). (b) Photograph of an injection site in the vIPAG. The microinjection sites were mostly distributed within the vIPAG region. Data from rats with an injection site outside of the vIPAG region were discarded. Aq: aqueduct of midbrain; vIPAG: ventrolateral periaqueductal gray.

Immunohistochemistry

The distribution of P2X₇ receptor in the vlPAG was detected using immunohistochemistry. The animals were sacrificed using an overdose of 4% chloral hydrate anesthesia (20 mL/kg body weight, i.p.) and perfused with 150 mL of normal saline (NS) in the aorta through the left ventricle followed by 200-mL of 4% paraformaldehyde in 0.2 M phosphate-buffered saline (PBS). The rats were decapitated, and their brains were rapidly removed, post-fixed in 4% paraformaldehyde/0.1 M PBS for 4–6 h, transferred to 30% sucrose for 48–60 h, and cryoprotected. PAGs were serially cut along the axis at a thickness of 25 μm by using a cryostat (Leica CM 1950, Germany). One of every five to six sections through the PAG was collected for immunohistochemical analysis. After incubation with 3% H₂O₂ in 0.01 M PBS and then 3% bovine serum albumin (BSA) in 0.1 M PBS, the sections were incubated with primary antibody (rabbit anti-rat P2X₇ polyclonal antiserum, 1:400; Abcam, USA) for P2X₇ receptors. After 1 h of incubation at 37°C, sections were stained overnight at 4°C. The 5% goat anti-rabbit serum (Beijing Zhongshan Biotech Co., China) was used as secondary antibody. Finally, the sections were mounted on glass slides, dehydrated through ascending series of ethanol solutions and xylene, and cover slipped. For confirming immune labeling specificity, control slides were exposed to diluted normal fetal bovine serum instead of the primary antibody. For quantification, images of positive staining in the vlPAG sections were analyzed using a Leica Q500IW image analysis system. Whole-mount preparations were used for quantitative analysis as described previously.⁴⁴ In brief, immunoreactive positive neuron bodies in the vlPAG were counted per visual field (0.3 mm²) in whole-mount preparations. Only cells with a distinct cell body and clear cellular boundary were included in the counts. Cell measurements were obtained from the mean value of five separate high-power fields per section, and 10 sections per brain were assayed. Cell density was expressed as cells per square millimeter with a 20× objective (total magnification 200×).

Western blot

For obtaining protein extracts, rats were sacrificed using an overdose of chloral hydrate (20 ml/kg body weight, i. p.) on day 21 after BCP operation, and whole PAGs were dissected and rapidly stored in a –70°C refrigerator. Before Western blot analysis, we attempted to harvest the vlPAG area, and the samples were sonicated in 400 μL of ice-cold lysis buffer (50 mM Tris–HCl [pH 7.5], 150 mM NaCl, 1% Triton X-100, 0.5% sodium deoxycholate, 0.1% sodium dodecyl sulfate (SDS), and 0.02% sodium azide) supplemented with proteinase

inhibitors. Protein concentrations of the lysate were determined using Bradford reagent (Bio-Rad, Hercules, CA, USA). For Western blot analysis, samples (20 μg of protein/lane) were loaded on a 12% SDS–polyacrylamide electrophoresis gel for 90 min at 120 V. After separation, the proteins were transferred to a polyvinylidene fluoride membrane for 6 h at 12 V. The membrane was shaken for 1 h at room temperature in Tris-buffered saline (TBS) containing 0.1% Tween-20, 5% skim milk, and 0.2% BSA. The membrane was incubated for 2 h at room temperature with primary antibody (1. rabbit polyclonal anti-P2X₇, Abcam Corporation, USA. 1:400; 2. mouse monoclonal anti-β-actin, Millipore Corporation, USA. 1:2000) in TBS containing 0.1% Tween-20. Immunoreactive proteins were detected by using enhanced chemiluminescence reagents (Pierce Biotechnology, Rockford, IL, USA) according to the manufacturer's instructions. The band intensity of the detected proteins was measured by using Quantity One software (Bio-Rad). Protein levels were normalized to β-actin as the loading control. Relative optical density (ROD) of the protein bands was measured after subtracting the film background. Data are expressed as mean ratio ± S.E.M of the P2X₇/β-actin protein.

Experimental design and drugs

The experiment consisted of four series. In series 1, we observed whether cancer cell inoculation, drug injection, or vlPAG microinjection exerted certain adverse effects on sensorimotor function in rats.

In series 2, we investigated the time-course changes of MWT or TWL values after the establishment of rat BCP model or intraperitoneal injection of different doses of tramadol. The rats were randomly and equally divided into the following six groups according to a random number table: normal, sham-BCP, BCP, T_L, T_M, and T_H groups (*n* = 12 per group). Pain threshold values were observed on postoperative days 0, 5, 7, 10, 14, 18, and 21. The T_L, T_M, and T_H group rats were intraperitoneally administered with 10, 20, and 40 mg/kg tramadol injection, respectively, once per day for 7 days from postoperative days 14 to 21.

In series 3, alterations of the P2X₇ receptor expression in the vlPAG were observed. A total of 12 rats from each group in series 2 were sacrificed on postoperative day 21, 6 rats were used for immunohistochemical analysis, and the other 6 rats were used for immunoblotting. Besides Western blot and immunohistochemical analysis, the tibia of each rat was harvested and observed by X-ray scanning and hematoxylin–eosin (HE) staining.

In series 4, the effects of pretreatment with A-740003 on the analgesic effect of 40 mg/kg tramadol (i.p. injection) was observed. In brief, 24 rats were randomly

divided into three groups ($n = 8$ per group), namely, BCP group, BCP rats with an i.p. injection of 40 mg/kg tramadol only (BCP+T_H group), and BCP rats with pretreatment of A-740003 30 min before i.p. injection of 40 mg/kg tramadol (BCP+T_H+A-740003 group).

Tramadol hydrochloride was purchased from DuoDuo Pharmaceutical Co., Ltd (Jiamusi, China), and A-740003 was obtained from Sigma-Aldrich. A-740003 was dissolved in NS solution and administered via intra-vIPAG injection in a volume of 100 nmol/0.3 μ L. Doses and treatment times of A-740003 were selected from our preliminary experiment or from previous studies. Antagonistic effect of A-740003 was assessed at 0, 15, 30, 45, 60, 75, and 90 min postmicroinjection.

Statistical analysis

Data were processed with the GraphPad Prism (version 6.01; GraphPad Software, Inc., CA). Results are expressed as mean \pm S.D. Statistical differences were assessed by one-way analysis of variance with a post hoc analysis for multiple comparisons. Student's *t*-test was used when only two independent groups were compared. A probability value of less than 0.05 indicates significant difference.

Results

Changes in sensorimotor function after BCP operation or drugs injection

Inclined plane test was used in all experimental rats before algometry test to study whether experimental procedures, e.g., modeling operation, drug microinjection, and i.p. injection exerted certain adverse effects on the sensorimotor function of the experimental rats. The average maximum angles at which a rat can retain its position were not significantly different among these groups (all $p > 0.05$, Figure 2).

Evaluation of bone destruction in BCP model

The BCP model was validated using radiological imaging and histological analysis. On day 21, postcancer cell inoculation on an X-ray picture of the rat tibia inoculated with SHZ-88 cells (ipsilateral) showed a loss of normal medullary cavity opacity and discontinuity of the bone structure, indicating bone destruction around the cancer cell injection site. No bone deficits were found on contralateral side tibia on day 21 postcancer cell inoculation (Figure 3(a) and (b)). Hematoxylin–eosin staining of tibia sections did not show cancer cells or bone destruction in the contralateral normal tibia of the BCP

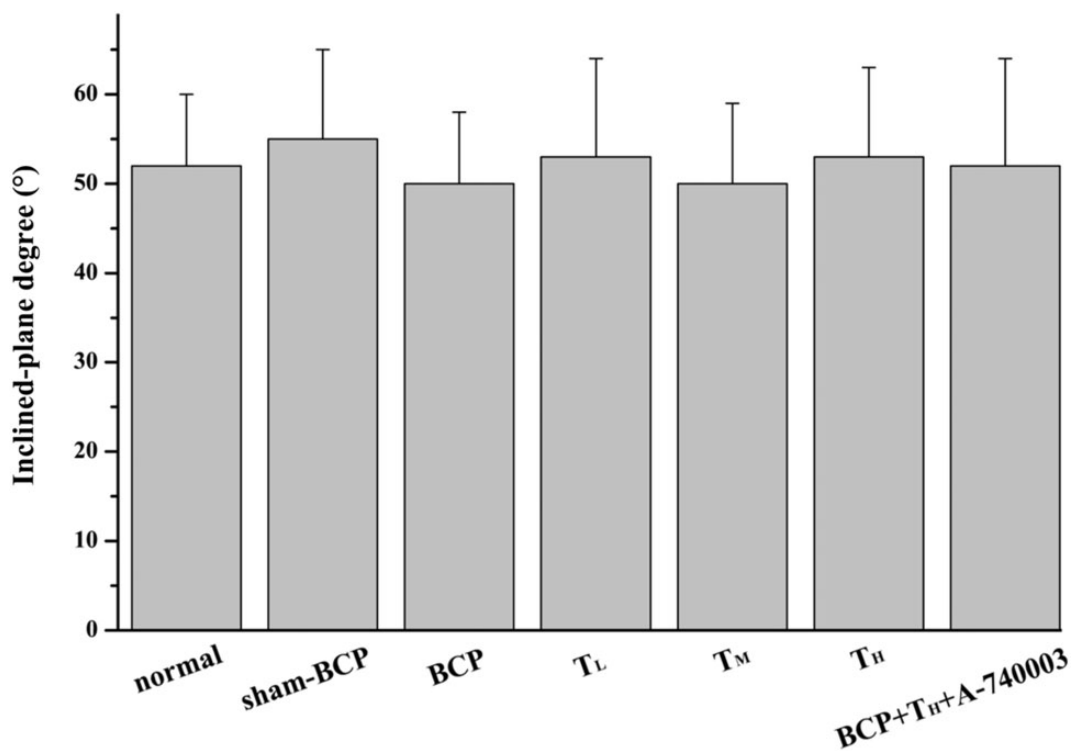


Figure 2. Changes in sensorimotor capability of the experimental rats. This histogram demonstrates the effect of experimental procedures on hind limb muscular strength and proprioception. Rats showed no considerable deficits in hind limb movement in this test. ($n = 12$ or 8). $p > 0.05$ among all groups. BCP: bone cancer pain.

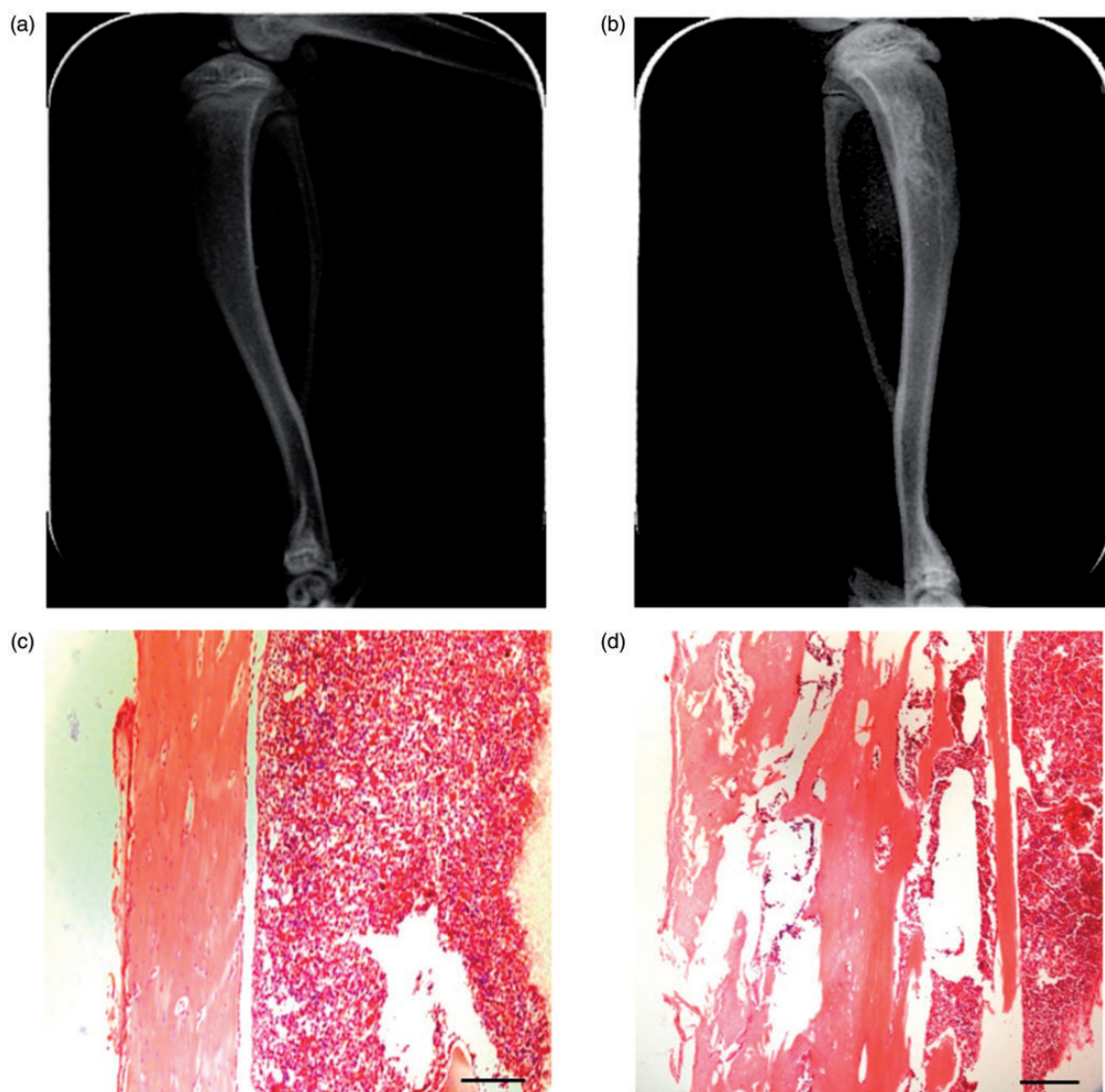


Figure 3. Tibia destruction at 21 days after SHZ-88 cell inoculation. Radiograph of the contralateral tibia shows an intact tibia, while ipsilateral tibia shows a loss of normal medullary cavity opacity and discontinuity of the bone structure in the tibia inoculated with cancer cells (a and b). Histopathological images of tibia sections stained by hematoxylin–eosin indicate obvious bone destruction along the surfaces of trabecular and compact bone (c and d). Scale bars = 250 μm . (a) Uninjured rat tibia (contralateral), (b) tibia bone cancer (ipsilateral), (c) contralateral side, and (d) ipsilateral side.

model rats (Figure 3(c) and (d)). However, the ipsilateral tibia showed marked bone destruction along the surfaces of trabecular and cortical bone, indicating the development of bone cancer in the tibia.

Alterations of pain thresholds by cancer cell inoculation

MWT was measured before BCP operation (day 0) and at days 5, 7, 10, 14, 18, and 21 post-operation. The mean MWT values of all groups of rats in the MWT test were approximately 39.41 g preoperatively. In the BCP group, hind paw MWT decreased from 38.69 ± 2.56 g before operation to 20.81 ± 2.17 g at day 10 ($p < 0.001$ compared

with that before cancer cell inoculation) and 11.47 ± 1.76 g at day 21 ($p < 0.001$ compared with that before cancer cell inoculation) after cancer cell inoculation. In the sham-BCP group, from day 5 to day 21 postcancer cell inoculation, the values of MWT were stable with no significant difference between sham-BCP and normal groups ($p > 0.05$). Changes in the TWL values exhibited a similar trend to that of MWT values (Figure 4(a) and (b)).

Changes of P2X₇ receptors expression in the vIPAG after cancer cell inoculation

The immunohistochemistry for P2X₇ receptors manifested weak and sparse P2X₇ receptor-specific immunoreactivity

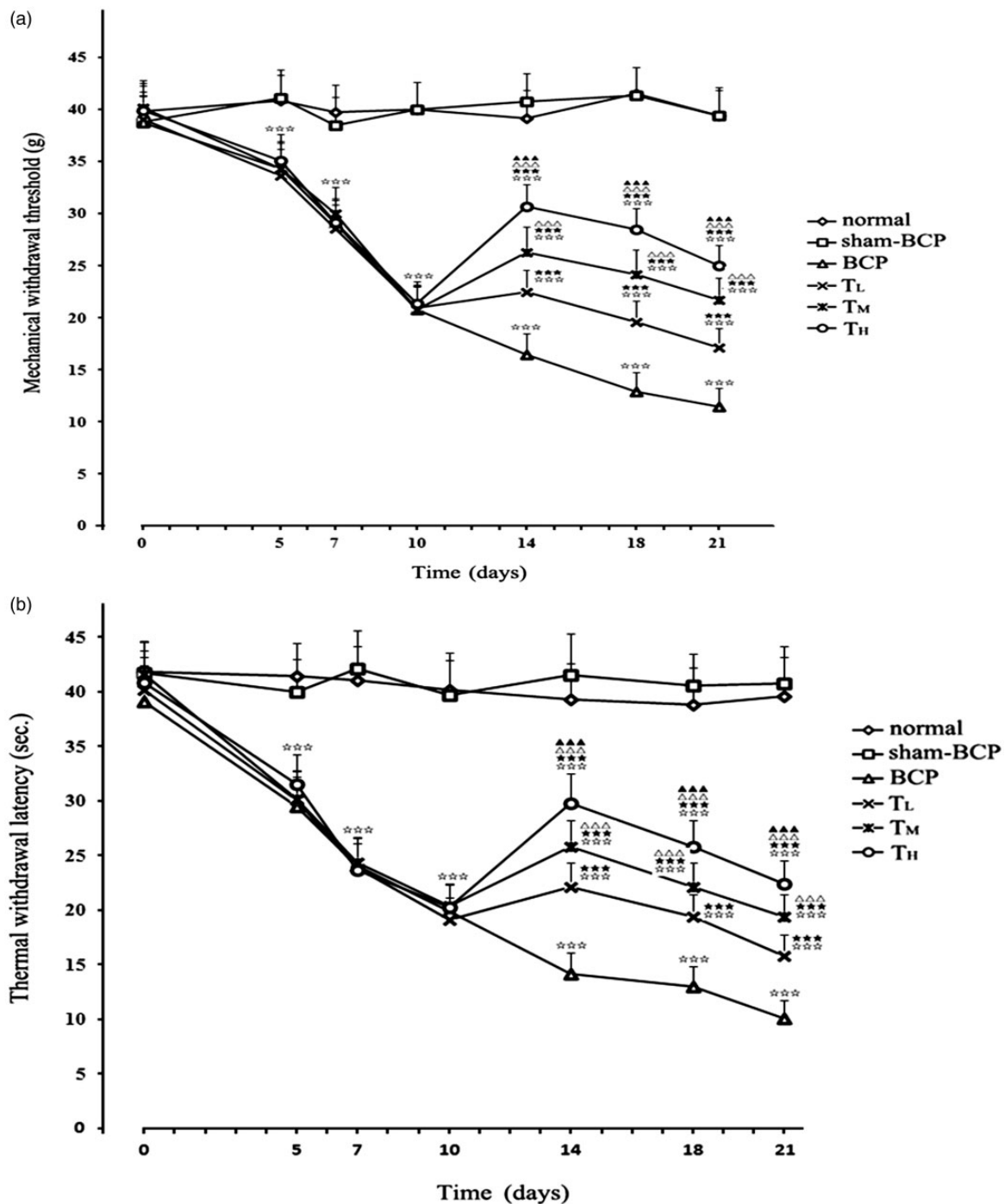


Figure 4. Cancer cell inoculation-induced mechanical and thermal hyperalgesia in rats. In the BCP group, cancer cell inoculation caused a significant decrease in MWT (a) or TWL (b) from day 5 to day 21 after BCP operation. The MWT and TWL values were significantly and dose dependently elevated after i.p. tramadol injection in T_L , T_M , and T_H groups. ($n = 12$). $☆☆☆p < 0.001$ versus sham-BCP group at the same time point; $***p < 0.001$ versus BCP group at the same time point; $\Delta\Delta\Delta p < 0.001$ versus T_L group at the same time point; $\blacktriangle\blacktriangle\blacktriangle p < 0.001$ versus T_M group at the same time point. BCP: bone cancer pain.

in vIPAG; that is, the $P2X_7$ -positive cell number for (637.26 ± 147.40) per mm^2 in the normal group and for (582.71 ± 134.15) per mm^2 in the sham-BCP group ($p > 0.05$, $n = 6$). In BCP groups (with $P2X_7$ -positive cell number of 730.53 ± 229.11 per mm^2), $P2X_7$

receptor-specific immunoreactivity was mildly increased compared with normal group or sham-BCP group on day 21 after BCP operation ($p < 0.05$, $n = 6$). Negative controls, with no primary antibody, did not show staining (Figure 5(a) and (b)).

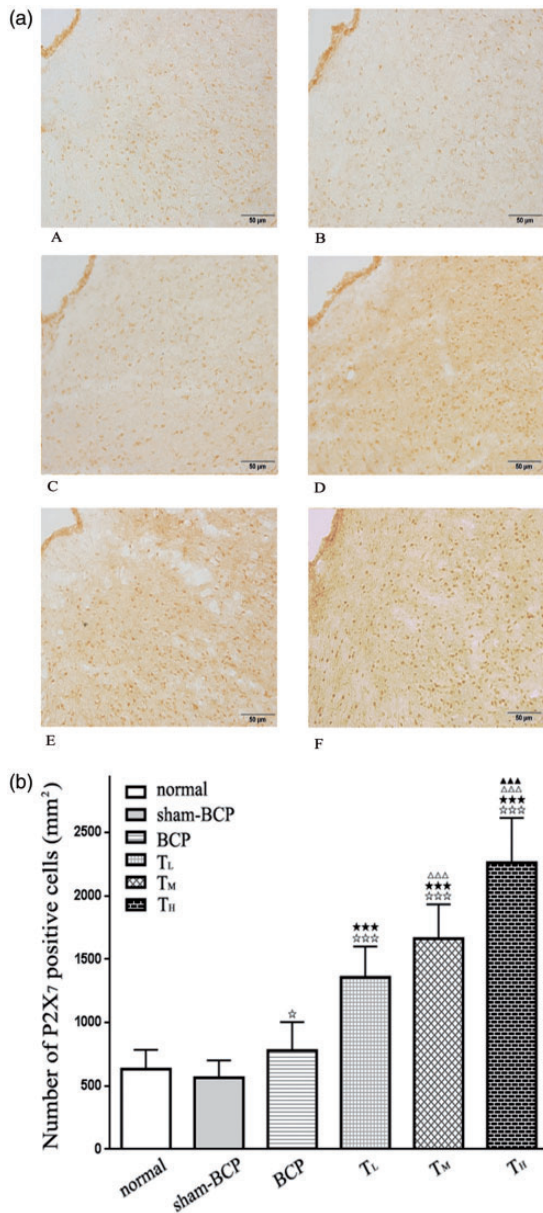


Figure 5. Changes of P2X₇ receptor expression in vIPAG following cancer cell inoculation or tramadol injections. (a) Photomicrographs are shown for P2X₇ receptor immunostaining in the vIPAG of normal group (Figure 5(a) A), sham-BCP group (Figure 5(a) B), BCP group (Figure 5(a) C), T_L group (Figure 5(a) D), T_M group (Figure 5(a) E), and T_H group (Figure 5(a) F). Scale bar = 50 μm. (b) The graph shows the number of P2X₇-positive cells in vIPAG. No distinct change in P2X₇ immunostaining was observed in vIPAG between normal and sham-BCP groups, but cancer cell inoculation upregulated the expression of P2X₇ receptor in vIPAG at day 21 after cancer cell inoculation in BCP group compared with normal and sham-BCP groups. Intraperitoneal tramadol injection at doses of 10, 20, and 40 mg/kg showed significantly and dose dependently upregulated the number of P2X₇-positive cells in vIPAG. (*n* = 6); **p* < 0.05 and ***p* < 0.001 compared with normal or sham-BCP group. ****p* < 0.001 versus BCP group; △△△*p* < 0.001 versus T_L group; ▲▲▲*p* < 0.001 versus T_M group. BCP: bone cancer pain.

Observation of P2X₇ receptor protein levels in vIPAG by Western blot analysis following cancer cell inoculation

Immunoblots from vIPAG homogenates revealed the presence of an immunopositive band of P2X₇ receptors with an apparent molecular weight of 68 kDa in normal, sham-BCP, and BCP groups. No significant difference was observed between normal (ROD: 82.45 ± 17.76) and sham-BCP groups (ROD: 90.23 ± 22.62) (*p* > 0.05). In the BCP group, cancer cell inoculation caused an increase in P2X₇ receptor protein level (ROD: 114.51 ± 28.89) compared with those in normal and sham-BCP rats at day 21 after BCP operation (all *p* < 0.01; *n* = 6; Figure 6(a) and (b)).

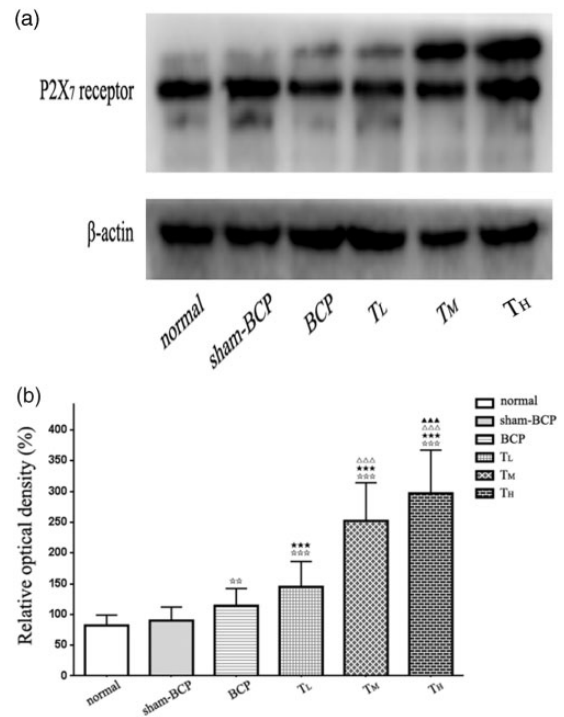


Figure 6. Alterations of P2X₇ receptor protein level in the vIPAG induced by cancer cell inoculation or tramadol injections. (a) By using Western blot analysis, we detected a protein band of ≈68 kDa, coinciding with the known molecular weight of the P2X₇ receptor. (b) β-actin was used as loading control. The P2X₇ receptor protein levels in different groups were expressed as ROD. No distinct change in P2X₇ receptor protein level was observed in vIPAG between normal and sham-BCP groups. The P2X₇ receptor protein level in vIPAG in BCP group was increased compared with normal and sham-BCP groups. Intraperitoneal tramadol injection at doses of 10, 20, and 40 mg/kg showed significantly and dose dependently upregulated the P2X₇ receptor protein level in vIPAG. (*n* = 6; ***p* < 0.01 and ****p* < 0.001 compared with normal or sham-BCP group. ****p* < 0.001 versus BCP group; △△△*p* < 0.001 versus T_L group; ▲▲▲*p* < 0.001 versus T_M group. BCP: bone cancer pain.

Effect of tramadol on hyperalgesia of BCP rats

No significant difference was observed in pain thresholds between BCP, T_L, T_M, and T_H groups on 10 days' post-cancer cell inoculation before i.p. tramadol injection ($p > 0.05$, $n = 12$). On 14 days' postcancer cell inoculation, the intraperitoneal administration of tramadol at doses of 10, 20, and 40 mg/kg considerably and dose dependently increased the MWT and TWL values of BCP rats compared with the pain threshold values of BCP group from 14 to 21 days' postcancer cell inoculation. Furthermore, the pain threshold values were significantly different among T_L, T_M, and T_H groups at the same time point (all $p < 0.001$; $n = 12$; Figure 4(a) and (b)).

Effect of tramadol on P2X₇ receptor expression on BCP rats

Compared with the BCP animals, rats administered with tramadol at doses of 10, 20, and 40 mg/kg once a day for 7 days significantly and dose dependently upregulated the number of P2X₇-positive cells in vlPAG at 21 days' postcancer cell inoculation ($p < 0.001$, $n = 6$; Figure 5(a) and (b)).

Effect of tramadol on P2X₇ protein level on BCP rats

Compared with BCP rats, rats administered with tramadol at doses of 10, 20, and 40 mg/kg once a day for 7 days significantly and dose dependently upregulated P2X₇ receptor protein levels in vlPAG at 21 days'

postcancer cell inoculation ($p < 0.001$, $n = 6$; Figure 6 (a) and (b)).

Influence of A-740003 pretreatments on the antinociceptive effect of i.p. injection of 40 mg/kg tramadol

In BCP+T_H+A-740003 group rats, MWT increased only from 11.98 ± 1.79 g to 20.02 ± 2.80 g, while TWL increased from 10.37 ± 1.09 s to 13.08 ± 1.77 s at 45 min after i.p. tramadol injection. The peak values of MWT and TWL were substantially lower than those of the T_H group ($p < 0.001$, compared with T_H group at the same time point), and the antinociceptive effect of tramadol was partially but significantly blocked by the vlPAG microinjection of P2X₇ receptor antagonist A-740003 (Figure 7(a) and (b)).

Discussion

In this study, a rat model for BCP was induced by inoculating SHZ-88 mammary gland carcinoma cells into the medullary cavity of the proximal tibia. The analgesic effects of i.p. injection of different doses of tramadol on BCP rats and the expression changes of P2X₇ receptor in vlPAG were observed. The main results of this study revealed that BCP rats exhibited a slight increased expression of P2X₇ receptor in vlPAG compared with normal rats. Tramadol (10, 20, and 40 mg/kg, i.p.) markedly and dose dependently ameliorated the pain behaviors of BCP rats, upregulated pain thresholds, and further raised the expression level of P2X₇ receptor in

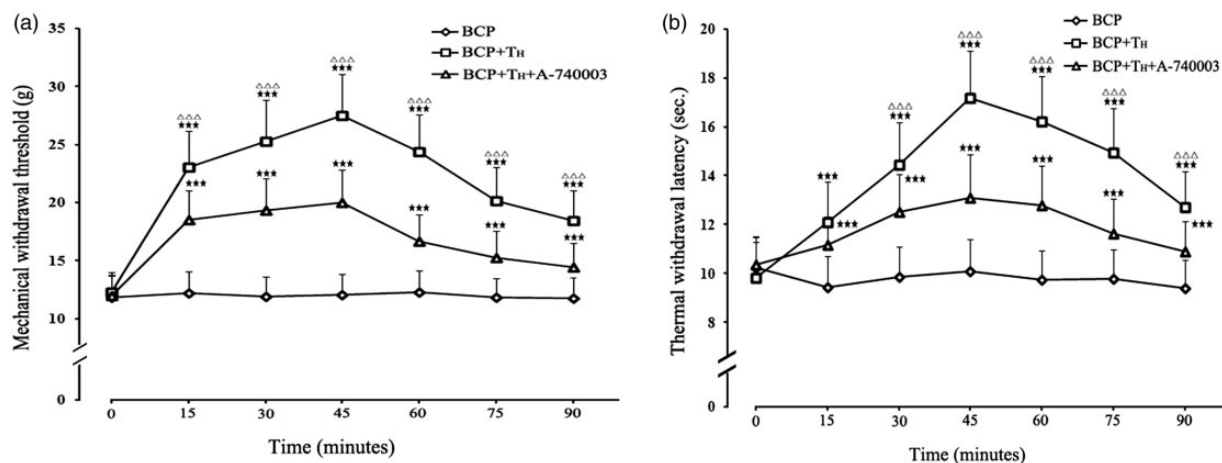


Figure 7. Pretreatment with A-740003 attenuates the antinociceptive effect of 40 mg/kg tramadol. The pain thresholds of each BCP rats before intra-vlPAG injection of A-740003 or i.p. tramadol injection served as control value ($p > 0.05$ among all groups). MWT (a) and TWL (b) values were significantly elevated after i.p. injection of 40 mg/kg tramadol, but pretreatment with A-740003 (100 nmol) intra-vlPAG injection attenuated the antinociceptive effect of 40 mg/kg tramadol in BCP rats. ($n = 8$). $***p < 0.001$, compared with the BCP group; $\Delta\Delta\Delta p < 0.001$, compared with the BCP+T_H+A-740003 group. BCP: bone cancer pain.

vIPAG. Intra-vIPAG microinjection of a selective P2X₇ receptor antagonist A-740003 partly but significantly reversed the analgesic effect of tramadol.

Using a mouse femur bone cancer (FBC) pain model, the researchers found that tramadol (100 mg/kg, s.c.) significantly decreased the retention time of FBC mice by a Rota-rod test,⁴⁵ meaning that tramadol at this dose can reduce the motor coordination capability of rats. In the current study, inclined-plane test was used in all experimental rats before algometry test to study whether BCP operation, drug administration, and intra-vIPAG microinjection exerted certain adverse effects on the motor function of experimental rats. The results showed all the experimental procedures without obvious effects on sensorimotor capability of the rats.

SHZ-88 carcinoma cell line was derived from rat breast carcinoma induced by dimethylbenzanthracene (DMBA). In the present study, when inoculated with 20 μ L (10⁷ cells/0.5 mL) SHZ-88 carcinoma cells, the rats survived for 30 and 40 days postinoculation, which allowed sufficient time to assess nociceptive activity. The measurement of nociceptive activity showed that activation threshold decreased considerably with respect to that of the sham-BCP group, thereby indicating mechanical allodynia. Moreover, thermal hyperalgesia was reported as determined as the decrease in retirement latency and compared with that of the sham-BCP group. The pain threshold values were usually reduced to a minimum at day 21; therefore, the X-ray images and HE staining were taken at day 21 postinoculation in this study. The radiographic results revealed a tumor growth with visible bone destruction, and histological images showed the destruction of smooth bone and trabecular bone of the tibia.

Cancer pain includes two components, namely, neuropathic pain and inflammatory pain. Notably, cancer pain also exhibits seemingly unique elements.^{6,46} ATP and its receptors play an important role in the formation and maintenance of pain.⁴⁷ The purine P2 receptor comprises a ligand-gated ion channel P2X receptor subtype and a G protein-coupled P2Y receptor subtype. P2X receptors and P2Y receptors are distributed on the surface of the cell membrane and are activated by extracellular ATP or other nucleotides that sequentially induce a series of physiological or pathophysiological changes. P2X receptors include seven subtypes (P2X₁₋₇) in which P2X₇ receptors are expressed predominantly in neurons and glial cells (microglia, astrocytes, and oligodendrocytes).⁴⁸⁻⁵⁰ Previous research has suggested the presence of P2X₇ receptor in the dorsal root ganglion and spinal cord dorsal horn and its involvement in neuropathic pain mechanism in rats.^{51,52} The studies suggested that P2X₇ receptors are involved in the modulation of neuropathic pain in relation to the following factors. (1) Purine signaling can be conducted by non-synaptic routes.

Preconditioning with ATP to the spinal cord slices of the neuropathic pain rats induce non-synaptic and non-neuronal P2X₇ receptor activation in the spinal cord, and increased glutamate release led to the formation of pain.⁵³ (2) P2X₇ receptor activation and Ca²⁺ influx activate a variety of downstream cell signal transduction pathways that excite sensory neurons, especially nociceptive neurons, thereby increasing their excitability and resulting in pain.⁵⁴ (3) Microglia P2X₇ receptors are involved in microglia and neuronal interactions (crosstalk). The activation of microglia P2X₇ receptors promotes interleukin-1 β (IL-1 β) release, phosphorylation of p38 mitogen-activated protein kinase, and the expression of glutamate receptor 1 (GluR1). Finally, the peripheral c fiber-induced field potential forms long-term potentiation, which leads to central sensitization and causes pain.⁵⁵ Likewise, P2X₇ receptor plays an important role in the modulation of inflammation, and inflammation reinforces the sensation of pain. The activation of P2X₇ receptor incurred an inflammatory response and subsequent release of inflammatory cytokines. By using antagonists of P2X₇ receptor, the inflammatory pain was obviously attenuated. Regrettably, the exact role of P2X₇ receptor in cancer pain currently remains controversial. Hansen et al.⁵⁶ discovered that P2X₇ receptor knockout mice were more vulnerable to BCP compared with cancer-bearing, wild-type mice. On the contrary, Huang et al.⁵⁷ demonstrated that the activation of microglial P2X₇ receptor in the rostral VMM contributes to the development of BCP via the upregulation of spinal 5-HT levels by the descending pain facilitatory system. Additionally, relatively few studies have reported on the role of P2X₇ receptors in pain regulation at the supraspinal anatomic sites at present. We demonstrated that the expression levels of P2X₇ receptor-positive cells and P2X₇ protein in vIPAG were considerably higher in BCP rats compared with those in sham BCP rats, indicating that tibia cancer cell inoculation may promote P2X₇ receptor expression in vIPAG.

Tramadol is used alone or in combination with other narcotics for neuropathic and inflammatory pain treatment.^{32,58} Several investigations revealed that tramadol can alleviate BCP in rodent models and in humans^{59,60}; however, these studies failed to correlate the mechanism underlying the analgesic effect of tramadol on BCP with the purinergic signaling pathway. Based on the previous findings,^{61,62} tramadol can rapidly penetrate the blood-brain barrier and blood-cerebrospinal fluid barrier. This study revealed that 10, 20, and 40 mg/kg tramadol i.p. administration caused a dose-dependent increase in the expression of P2X₇ receptor in vIPAG compared with that in BCP rats. The classical view of tramadol analgesic mechanisms includes two main routes: (1) playing an analgesic role by activating the central opiate receptor

(mainly μ receptor) and (2) inhibiting the re-uptake of NE and serotonin (5-HT), which increase NE and 5-HT levels in the synaptic cleft when released from the nerve endings. Tramadol is a racemic mixture with a molecular structure containing two optical enantiomers. The drug exerts analgesic effect through different mechanisms, namely, dextrose tramadol activation of the opioid μ receptor and left-enantiomer inhibition of NE and 5-HT re-uptake.³⁵ On one hand, Gordon et al.⁶³ found that in rat hypothalamic paraventricular nucleus, NE can promote glial cell release of ATP; combined with the current study, we deduced that i.p. injection of tramadol possibly reduces NE re-uptake in vIPAG and thus increases NE levels in the local microenvironment, consequently increasing the ATP level and upregulating P2X₇ receptor expression in vIPAG; on the other hand, Papp et al.⁶⁴ found that P2X_{1, 2, 3, 4, 6, 7} receptors expressed on the brainstem catecholaminergic neurons project to the hippocampus and that the activation of the above P2X receptor enhance NE release. From the above-mentioned reasons, there may be existed a cross-talk between NE and ATP. In our previous study, we observed up-regulation of P2X₃ receptors in vIPAG in neuropathic pain rats.⁶⁵ Thus, we hypothesized that a similar mechanism may exist in vIPAG in BCP rats, that is, P2X₃ receptors in BCP rats are activated, and NE release increases and further promote ATP release, ultimately leading to P2X₇ receptor activation. The hypotheses need to be further validated.

Yuan et al.⁵⁹ found that i.p. injection of tramadol (10 mg/kg) can relieve BCP in rats. Our results showed that i.p. injections of tramadol exert a dose-dependent analgesic effect on BCP rats, and this analgesic effect was reversed by intra-vIPAG injection of a selective P2X₇ receptor antagonist A-740003. Known tramadol analgesia mechanisms involve multiple neurotransmitter systems, such as opioid, NE, and 5-HT systems, which are closely related to pain.^{34,66} To the best of our knowledge, no research has determined the relationship between tramadol and purine receptors to date. This study further clarifies that the purine signaling pathway is also involved in the tramadol analgesic mechanism. Therefore, the current study can further our understanding of the interaction between pain-related neurotransmitters.

In summary, the present study demonstrates that the i.p. injection of tramadol enhances P2X₇ receptor activation in the vIPAG and exerts a dose-dependent analgesic effect on BCP. These findings suggest that the activation of purine P2X₇ receptor in vIPAG is involved in the analgesic mechanism of tramadol, thus providing theoretical basis for the clinical application of tramadol and potential for the development of new drugs targeting P2X₇ receptors.

Author contributions

PT, QZ, ZX, SY, YQ, and YY performed the experiments. ZX analyzed the data and drafted the manuscript. All authors read and approved the final version of the manuscript.

Acknowledgments

The authors thank Wei Chen and Xiang Lu for their support with the histological analysis work.

Declaration of Conflicting Interests

The author(s) declared no potential conflicts of interest with respect to the research, authorship, and/or publication of this article.

Funding

The author(s) disclosed receipt of the following financial support for the research, authorship, and/or publication of this article: The study was supported by the National Natural Science Foundation of China (grant number 81760214 to Zhi Xiao) and Guizhou Provincial Science and Technology Planning Project (grant number QianKeHe JiChu [2017]1214 to Zhi Xiao).

References

- Mantyh PW. Bone cancer pain: from mechanism to therapy. *Curr Opin Support Palliat Care* 2014; 8: 83–90.
- Leppert W, Zajackowska R, Wordliczek J, Dobrogowski J, Woron J and Krzakowski M. Pathophysiology and clinical characteristics of pain in most common locations in cancer patients. *J Physiol Pharmacol* 2016; 67: 787–799.
- Kane CM, Hoskin P and Bennett MI. Cancer induced bone pain. *BMJ* 2015; 350: h315
- Mantyh P. Bone cancer pain: causes, consequences, and therapeutic opportunities. *Pain* 2013; 154 Suppl 1: S54–S62.
- Zhu YF, Ungard R, Seidlitz E, Zagal N, Huizinga J, Henry JL and Singh G. Differences in electrophysiological properties of functionally identified nociceptive sensory neurons in an animal model of cancer-induced bone pain. *Mol Pain* 2016; 12: 174480691662877.
- Figura N, Smith J and Yu HM. Mechanisms of, and adjuvants for, bone pain. *Hematol Oncol Clin North Am* 2018; 32: 447–458.
- Hua B, Gao Y, Kong X, Yang L, Hou W and Bao Y. New insights of nociceptor sensitization in bone cancer pain. *Expert Opin Ther Targets* 2015; 19: 227–243.
- Zhou Y-Q, Liu Z, Liu H-Q, Liu D-Q, Chen S-P, Ye D-W and Tian Y-K. Targeting glia for bone cancer pain. *Expert Opin Ther Targets* 2016; 20: 1365–1374.
- Inoue K. ATP receptors of microglia involved in pain. *Novartis Found Symp* 2006; 276: 263–272. discussion 273–281.
- Chwistek M. Recent advances in understanding and managing cancer pain. *F1000Res* 2017; 6: 945.
- Zhou Y-Q, Chen S-P, Liu D-Q, Manyande A, Zhang W, Yang S-B, Xiong B-R, Fu Q-C, Song Z-P, Rittner H, Ye D-W and Tian Y-K. The role of spinal GABAB

- receptors in cancer-induced bone pain in rats. *J Pain* 2017; 18: 933–946.
12. Liu M, Yao M, Wang H, Xu L, Zheng Y, Huang B, Ni H, Xu S, Zhou X and Lian Q. P2Y₁₂ receptor-mediated activation of spinal microglia and p38MAPK pathway contribute to cancer-induced bone pain. *J Pain Res* 2017; 10: 417–426.
 13. Portenoy RK. Treatment of cancer pain. *Lancet* 2011; 377: 2236–2247.
 14. Burnstock G. Purinergic signalling: pathophysiology and therapeutic potential. *Keio J Med* 2013; 62: 63–73.
 15. Burnstock G and Kennedy C. P2X receptors in health and disease. *Adv Pharmacol* 2011; 61: 333–372.
 16. Nobile M, Monaldi I, Alloisio S, Cugnoli C and Ferroni S. ATP-induced, sustained calcium signalling in cultured rat cortical astrocytes: evidence for a non-capacitative, P2X₇-like-mediated calcium entry. *FEBS Lett* 2003; 538: 71–76.
 17. Di Virgilio F, Chiozzi P, Ferrari D, Falzoni S, Sanz J M, Morelli A, Torboli M, Bolognesi G and Baricordi OR. Nucleotide receptors: an emerging family of regulatory molecules in blood cells. *Blood* 2001; 97: 587–600.
 18. Barros-Barbosa AR, Lobo MG, Ferreirinha F, Correia-de-Sá P and Cordeiro JM. P2X₇ receptor activation downmodulates Na(+)-dependent high-affinity GABA and glutamate transport into rat brain cortex synaptosomes. *Neuroscience* 2015; 306: 74–90.
 19. Burnstock G and Knight GE. The potential of P2X₇ receptors as a therapeutic target, including inflammation and tumour progression. *Purinergic Signal* 2018; 14: 1–18.
 20. Hughes JP, Hatcher JP and Chessell IP. The role of P2X₇ in pain and inflammation. *Purinergic Signal* 2007; 3: 163–169.
 21. Burnstock G. Purinergic mechanisms and pain. *Adv Pharmacol* 2016; 75: 91–137.
 22. Bernier LP, Ase AR and Seguela P. P2X receptor channels in chronic pain pathways. *Br J Pharmacol* 2018; 175: 2219–2230.
 23. Tavares I and Lima D. From neuroanatomy to gene therapy: searching for new ways to manipulate the supraspinal endogenous pain modulatory system. *J Anat* 2007; 211: 261–268.
 24. Millan MJ. Descending control of pain. *Prog Neurobiol* 2002; 66: 355–474.
 25. Behbehani MM. Functional characteristics of the midbrain periaqueductal gray. *Prog Neurobiol* 1995; 46: 575–605.
 26. Mills EP, Di Pietro F, Alshelhi Z, Peck CC, Murray GM, Vickers ER and Henderson LA. Brainstem pain-control circuitry connectivity in chronic neuropathic pain. *J Neurosci* 2018; 38: 465–473.
 27. Worthington RA, Arumugam TV, Hansen MA, Balcar VJ and Barden JA. Identification and localisation of ATP P2X receptors in rat midbrain. *Electrophoresis* 1999; 20: 2077–2080.
 28. Xiao Z, Li YY and Sun MJ. Activation of P2X receptors in the midbrain periaqueductal gray of rats facilitates morphine tolerance. *Pharmacol Biochem Behav* 2015; 135: 145–153.
 29. Gao X-F, Wang W, Yu Q, Burnstock G, Xiang Z-H and He C. Astroglial P2X₇ receptor current density increased following long-term exposure to rotenone. *Purinergic Signal* 2011; 7: 65–72.
 30. Mintzer MZ, Lanier RK, Lofwall MR, Bigelow GE and Strain EC. Effects of repeated tramadol and morphine administration on psychomotor and cognitive performance in opioid-dependent volunteers. *Drug Alcohol Depend* 2010; 111: 265–268.
 31. Montero Matamala A, Bertolotti M, Contini MP, Guerrero Bayón C, Nizzardo A, Paredes Lario I, Pizà Vallespir B, Scartoni S, Tonini G, Capriati A and Pellacani A. Tramadol hydrochloride 75 mg/dexketoprofen 25 mg oral fixed-dose combination in moderate-to-severe acute pain: sustained analgesic effect over a 56-h period in the postoperative setting. *Drugs Today* 2017; 53: 339–347.
 32. Nishikawa N and Nomoto M. Management of neuropathic pain. *J Gen Fam Med* 2017; 18: 56–60.
 33. Hassamal S, Miotto K and Dale W. Tramadol: understanding the risk of serotonin syndrome and seizures. *Am J Med*. Epub ahead of print 10 May 2018. DOI: 10.1016/j.amjmed.2018.04.025.
 34. Miotto K, Cho AK, Khalil MA, Blanco K, Sasaki JD and Rawson R. Trends in tramadol: pharmacology, metabolism, and misuse. *Anesth Analg* 2017; 124: 44–51.
 35. Beakley BD, Kaye AM and Kaye AD. Tramadol, pharmacology, side effects, and serotonin syndrome: a review. *Pain Physician* 2015; 18: 395–400.
 36. Zimmermann M. Ethical guidelines for investigations of experimental pain in conscious animals. *Pain* 1983; 16: 109–110.
 37. Pérez-Rojas JM, González-Macías R, González-Cortés J, Jurado R, Pedraza-Chaverri J and García-López P. Synergic effect of alpha-mangostin on the cytotoxicity of cisplatin in a cervical cancer model. *Oxid Med Cell Longev* 2016; 2016: 1.
 38. Shenoy PA, Kuo A, Vetter I and Smith MT. The walker 256 breast cancer cell- induced bone pain model in rats. *Front Pharmacol* 2016; 7: 286.
 39. Liu H, Zhu R, Liu C, Ma R, Wang L, Chen B, Li L, Niu J, Zhao D, Mo F, Fu M, Brömme D, Zhang D and Gao S. Evaluation of decalcification techniques for rat femurs using HE and immunohistochemical staining. *Biomed Res Int* 2017; 2017: 1.
 40. Paxinos G and Watson C. *The rat brain in stereotaxic coordinates*. 6th ed. Amsterdam, The Netherlands: Academic Press, 2007.
 41. Rivlin AS and Tator CH. Objective clinical assessment of motor function after experimental spinal cord injury in the rat. *J Neurosurg* 1977; 47: 577–581.
 42. Cunha TM, Verri WA Jr, Vivancos GG, Moreira IF, Reis S, Parada CA, Cunha FQ and Ferreira SH. An electronic pressure-meter nociception paw test for mice. *Braz J Med Biol Res* 2004; 37: 401–407.
 43. Hargreaves K, Dubner R, Brown F, Flores C and Joris J. A new and sensitive method for measuring thermal nociception in cutaneous hyperalgesia. *Pain* 1988; 32: 77–88.
 44. Van Nassauw L, Bogers J, Van Marck E and Timmermans JP. Role of reactive nitrogen species in neuronal cell

- damage during intestinal schistosomiasis. *Cell Tissue Res* 2001; 303: 329–336.
45. Ono H, Nakamura A, Kanbara T, Minami K, Shinohara S, Sakaguchi G and Kanemasa T. Effect of the norepinephrine transporter (NET) inhibition on mu-opioid receptor (MOR)-induced anti-nociception in a bone cancer pain model. *J Pharmacol Sci* 2014; 125: 264–273.
 46. Falk S and Dickenson AH. Pain and nociception: mechanisms of cancer-induced bone pain. *J Clin Oncol* 2014; 32: 1647–1654.
 47. Burnstock G. Purinergic mechanisms and pain—an update. *Eur J Pharmacol* 2013; 716: 24–40.
 48. Miras-Portugal MT, Sebastián-Serrano Á, de Diego García L and Díaz-Hernández M. Neuronal P2X7 receptor: involvement in neuronal physiology and pathology. *J Neurosci* 2017; 37: 7063–7072.
 49. Bhattacharya A and Biber K. The microglial ATP-gated ion channel P2X7 as a CNS drug target. *Glia* 2016; 64: 1772–1787.
 50. Rivera A, Vanzulli I and Butt AM. A central role for ATP signalling in glial interactions in the CNS. *Curr Drug Targets* 2016; 17: 1829–1833.
 51. Yang J, Park KS, Yoon JJ, Bae H-B, Yoon MH and Choi JI. Anti-allodynic effect of intrathecal processed Aconitum jaluense is associated with the inhibition of microglial activation and P2X7 receptor expression in spinal cord. *BMC Complement Altern Med* 2016; 16: 214.
 52. Xie J, Liu S, Wu B, Li G, Rao S, Zou L, Yi Z, Zhang C, Jia T, Zhao S, Schmalzing G, Hausmann R, Nie H, Li G and Liang S. The protective effect of resveratrol in the transmission of neuropathic pain mediated by the P2X7 receptor in the dorsal root ganglia. *Neurochem Int* 2017; 103: 24–35.
 53. Ando RD and Sperlagh B. The role of glutamate release mediated by extrasynaptic P2X7 receptors in animal models of neuropathic pain. *Brain Res Bull* 2013; 93: 80–85.
 54. Sperlagh B, Vizi ES, Wirkner K and Illes P. P2X7 receptors in the nervous system. *Prog Neurobiol* 2006; 78: 327–346.
 55. Chu Y-X, Zhang Y, Zhang Y-Q and Zhao Z-Q. Involvement of microglial P2X7 receptors and downstream signaling pathways in long-term potentiation of spinal nociceptive responses. *Brain Behav Immun* 2010; 24: 1176–1189.
 56. Hansen RR, Nielsen CK, Nasser A, Thomsen SIM, Eghorn LF, Pham Y, Schulenburg C, Syberg S, Ding M, Stojilkovic SS, Jorgensen NR and Heegaard A-M. P2X7 receptor-deficient mice are susceptible to bone cancer pain. *Pain* 2011; 152: 1766–1776.
 57. Huang ZX, Lu ZJ, Ma WQ, Wu FX, Zhang YQ, Yu W-F and Zhao ZQ. Involvement of RVM-expressed P2X7 receptor in bone cancer pain: mechanism of descending facilitation. *Pain* 2014; 155: 783–791.
 58. Mert T, Sahin E and Yaman S. Pain-relieving effectiveness of co-treatment with local tramadol and systemic minocycline in carrageenan-induced inflammatory pain model. *Inflammation* 2018; 41: 1238–1249.
 59. Yuan X, Wu J, Wang Q and Xu M. The antinociceptive effect of systemic administration of a combination of low-dose tramadol and dexmedetomidine in a rat model of bone cancer pain. *Eur J Anaesthesiol* 2014; 31: 30–34.
 60. Corona-Ramos JN, Déciga-Campos M, Romero-Piña M, Medina LA, Martínez-Racine I, Jaramillo-Morales OA, García-López P and López-Muñoz FJ. The effect of gabapentin and tramadol in cancer pain induced by glioma cell in rat femur. *Drug Dev Res* 2017; 78: 173–183.
 61. Sheikholeslami B, Gholami M, Lavasani H and Rouini M. Evaluation of the route dependency of the pharmacokinetics and neuro-pharmacokinetics of tramadol and its main metabolites in rats. *Eur J Pharm Sci* 2016; 92: 55–63.
 62. Kitamura A, Higuchi K, Okura T and Deguchi Y. Transport characteristics of tramadol in the blood-brain barrier. *J Pharm Sci* 2014; 103: 3335–3341.
 63. Gordon GRJ, Baimoukhametova DV, Hewitt SA, Rajapaksha WRAKJS, Fisher TE and Bains JS. Norepinephrine triggers release of glial ATP to increase postsynaptic efficacy. *Nat Neurosci* 2005; 8: 1078–1086.
 64. Papp L, Balázs T, Köfalvi A, Erdélyi F, Szabó G, Vizi ES and Sperlagh B. P2X receptor activation elicits transporter-mediated noradrenaline release from rat hippocampal slices. *J Pharmacol Exp Ther* 2004; 310: 973–980.
 65. Xiao Z, Ou S, He W-J, Zhao Y-D, Liu X-H and Ruan H-Z. Role of midbrain periaqueductal gray P2X3 receptors in electroacupuncture-mediated endogenous pain modulatory systems. *Brain Res* 2010; 1330: 31–44.
 66. Bravo L, Mico JA and Berrocoso E. Discovery and development of tramadol for the treatment of pain. *Expert Opin Drug Discov* 2017; 12: 1281–1291.